Multi-modal calibration of surveillance sensor networks

Min Ding
Computer Science Department
George Washington University
Washington
DC 20052, USA

Andreas Terzis
Computer Science Department
Johns Hopkins University
Baltimore
MD 21218, USA

I-Jeng Wang Dennis Lucarelli
Applied Physics Lab
Johns Hopkins University
Laurel
MD 20723, USA

June 13, 2006

Abstract

Target detection and localization is one of the key research challenges in sensor networks. In this paper we propose a heterogeneous wireless sensor network integrating imaging and non-imaging sensors to accomplish the detection and localization task in complex urban environments. The low-cost non-imaging sensors provide early detection and partial localization of potential targets and direct imaging sensors to focus on them. Accurate target location estimated by the imaging sensors is then used to calibrate the non-imaging sensors.

We evaluate our approach through simulation and implementation on a sensor network testbed that uses MicaZ motes equipped with magnetometers and a camera to track ferrous targets. Our preliminary results reveal that coordination across different sensing modalities increases localization accuracy and reduces the amount of imaging data that has to be processed by the network.

1 Introduction

Using network of sensor devices for surveillance missions is to acquire, process and extract information from deployed and unmanned heterogeneous sensors in all kinds of environment. This is of great practical importance for the military.

Such a network can provide a fine global picture through the collaboration of many sensors with each observing a coarse local view [6]. With their capabilities for distributed sensing and in-network processing, networked sensors are expected to be widely deployed and to perform some decentralized information processing tasks such as environmental monitoring, disaster recovery and urban rescue, target identification and tracking. The difficulty in flourishing these networks lies in in-network processing observations from sensors in close geographic proximity [4].

In this paper we propose a heterogeneous wireless sensor network integrating imaging and non-imaging sensors to accomplish the detection and localization task in complex urban environments that is one of the key research challenges in sensor networks. Particularly, we employ magnetometers to find the coarse locations of targets within our sensing range, then utilize these information guiding the camera sensor to compute the more precise target positions, finally calibrate the magnetometers' reading parameters using nonlinear least-square technique based on detected accurate target locations. We validate our method with both simulation data and a real sensor network system deployed in our laboratory. In simulation, our experimental results demonstrate that the estimated magnetometers' sensing parameters converges to the real values under low to moderate levels of camera noise, and the calibration results can be improved with larger number of magnetometers.

Our paper is organized as follows. We first illustrate the motivation of proposing a heterogeneous sensor network for target detection and tracking, then our detail algorithm design is presented in section 3. Using simulation data under controlled conditions, our method is empirically validated and performance evaluated using our in section 4, which is followed by the experiments from our real sensornet system deployed in a real complex environment. Finally we conclude the paper and discuss the future extension and improvement.

2 Motivation

In Figure 1, we illustrate an example of our system working scenario. We present a heterogenous sensing framework to solve target detection, location and tracking in real environment. Direct imaging sensor, such as a surveillance camera, can compute the target location with high precision, but has a limited field-of-view and can not be deployed everywhere. Thus it may have many blind-spots in the field lack-

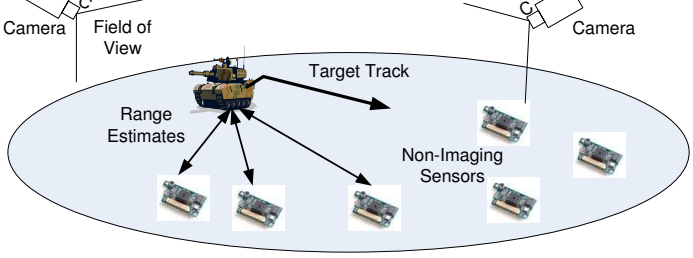

Figure 1: Multi-modal sensor network for target tracking.

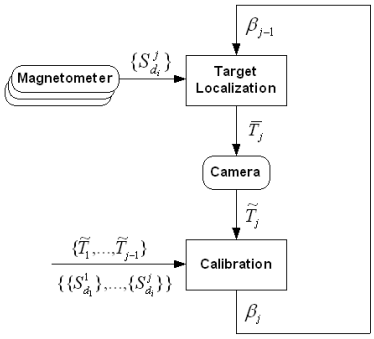

Figure 2: Block diagram of the proposed target tracking system.

ing of sensing ability. However our low-cost magnetometers, or other types of non-imaging sensors, can form a densely distributed wireless network in a large range of environment. They can be used to find target covering the whole surveillance field, but with limited localization accuracy. In a collaborative manner, the non-imaging sensors in our system can first detect and estimate the coarse target position; then report and guide imaging sensor's field-of-view to further localize target's position accurately; finally the more precise target locations can also help to calibrate non-imaging sensors' reading parameters for improved coarse-level target localization in the next stage.

Challenges

3 Design

3.1 Overview

We propose a unified approach by iteratively calibrating sensor parameters and optimizing the target locations overtime.

Figure 2 illustrates our unified framework for calibration and target localization that includes both non-imaging sensor

ical position through either GPS or GPS-less techniques [3]. We assume the sensors can then detect the target presence and report their readings $\{S^j_{d_i}\}$, where $S^j_{d_i}$ is the sensor s_i's reading for target at location T_j, to the base station. Based on the sensor readings, the base station estimates the target locations $\bar{T}_j$ in the global coordinates through *our collaborative localization algorithm* and guides the camera to track the target. Furthermore the sensor reading parameters β_j can also be calibrated from the estimated target positions using *the nonlinear least square* consequently. As the target moves, the current calibrated parameters are input to the localization module to predict target's location more accurately, and then the sequential target location observations from imaging sensor can improve the calibration accuracy of sensor parameters and readings as well. Our method results in an iterative optimization on $\bar{T}_j$ and β_j overtime.

In the following, we describe our mathematical formulation of sensor parameter calibration and target localization algorithms.

3.2 Localization

Calibration Model: We assume the signal strength propagate according to the ideal decay function as shown in the following equation:

$$S_d = S_T / d^\beta, \tag{1}$$

where S_T is a constant describes the original signal power, S_d is the measured signal strength at distance d, and β is the decay factor.

The signal strength measured at a sensor follows the following equation

$$S_d = S_T / d^\beta + \mathcal{N}_1, \tag{2}$$

where $\mathcal{N}_1$ is a zero mean white noise satisfying Gaussian distribution. In some application, we do not know what kind of target will present and the value of S_T is unknown. The decay factor β is determined by the environment. We need to figure out how to estimate accurate β in different situation. Its accuracy influences the result of target localization.

Localization Strategy: We propose a heterogeneous wireless sensor network integrating imaging and non-imaging sensors to accomplish the detection and localization task in complex urban environments. The low-cost non-imaging sensors provide early detection and partial localization of potential targets and direct imaging sensors to focus on them. Accurate target location estimated by the imaging sensors is then used to calibrate the non-imaging sensors.

Unified Optimization: Given a group of pairs of $(\tilde{d}_i, S_{d_i})$, where $\tilde{d}_i$ is the distance from a sensor s_i around the target to the camera located target and S_{d_i} is the signal measurement at that sensor, we attempt to find the value of β which best satisfy Eq. (1). This problem can be formulated as a nonlinear least square problem which is numerically solved by gradient descent optimization, given an initial β. We try to minimize the cost function

$$\sum (S_{d_i} - S_T/\tilde{d}_i^{\beta})^2. \tag{3}$$

Assume that the target position obtained from camera $\tilde{d}_i$ has additive zero mean Gaussian noise $\mathcal{N}_2$. As the target moves, we collect more measurements from sensor readings as groups of $(\tilde{d}_i^j, S_{d_i}^j)$, where $\tilde{d}_i^j$ is the distance from the ith sensor to the camera located target position at $\tilde{T}_j$.

To evaluate the accuracy of estimated $\bar{\beta}$, we use S_T, sensor readings $S_{d_i}^j$ $(i = 3, ..., 8)$ and $\bar{\beta}$ to compute the target location $\bar{T}_j$ by least squares fitting. Let $[x_i, y_i]$ and $[\bar{X}_{T_j}, \bar{Y}_{T_j}]$ denote the sensor s_i and target $\bar{T}_j$'s coordinates. By transforming the signal strength propagation model, ie. equation 1, we can get the distance $\bar{d}_i^j$ from the ith sensor to target location $\bar{T}_j$ by the following equation,

$$\bar{d}_i^j = \sqrt[\bar{\beta}]{\frac{S_T}{S_{d_i}^j}}. \tag{4}$$

Then we can estimate $[\bar{X}_{T_j}, \bar{Y}_{T_j}]$ from a group of equations

$$(x_i - \bar{X}_{T_j})^2 + (y_i - \bar{Y}_{T_j})^2 = (\bar{d}_i^j)^2, i = 1, ..., I; I = 3, ..., 8. \tag{5}$$

For example, if there exist three sensors for the target, we will try to solve the following equations for $[\bar{X}_{T_j}.\bar{Y}_{T_j}]$

$$(x_1 - \bar{X}_{T_j})^2 + (y_1 - \bar{Y}_{T_j})^2 = (\bar{d}_1^j)^2, \tag{6}$$

$$(x_2 - \bar{X}_{T_j})^2 + (y_2 - \bar{Y}_{T_j})^2 = (\bar{d}_2^j)^2, \tag{7}$$

$$(x_3 - \bar{X}_{T_j})^2 + (y_3 - \bar{Y}_{T_j})^2 = (\bar{d}_3^j)^2, \tag{8}$$

To avoid the nonlinearity of the above equations, we can subtract any equation to another. For example, if subtracting Eq. (6) from Eq. (7), we obtain

$$\begin{aligned} 2(x_2 - x_1)\bar{X}_{T_j} + 2(y_2 - y_1)\bar{Y}_{T_j} = ((\bar{d}_1^j)^2 - x_1^2 - y_1^2) \\ -((\bar{d}_2^j)^2 - x_2^2 - y_2^2). \end{aligned} \tag{9}$$

From I Eq.5 type equations, we can have $I - 1$ linearly independent equations where $(I - 1) >= 2$ guaranteeing the following linear equations to solve $[\bar{X}_{T_j}, \bar{Y}_{T_j}]$.

$$\begin{aligned} 2(x_i - x_1)\bar{X}_{T_j} + 2(y_i - y_1)\bar{Y}_{T_j} = ((\bar{d}_1^j)^2 - x_1^2 - y_1^2) \\ -((\bar{d}_i^j)^2 - x_i^2 - y_i^2), i = 2, ..., I; I = 3, ..., 8. \end{aligned} \tag{10}$$

Finally, $[\bar{X}_{T_j}, \bar{Y}_{T_j}]$ can be solved from Eq. (10) by linear least squares fitting with 3 or more sensors.

4 Evaluation

We first use Matlab to implement our algorithms with controlled simulation to validate the approach. Realtime live demonstration with onboard sensors is under implementation.

To simulate the parameter estimation process with multimodal calibration, we assume the target moves with a stable speed in a straight line in $X-Y$ plane. Some sensor nodes are then randomly deployed within at least 1 and at most 4 distance units to the target. Assume that the target signal power S_T is known and the sensor network is synchronized. Each sensor node knows its own position. The sensors receive signal strengths according to the Eq. 2.

Using simulation data under controlled conditions make it feasible to validate our method qualitatively, and evaluate the performance quantitatively. In the following, we focus on analyzing two quantitative metrics: the convergent speed and accuracy of β to the real setting and the resulting target location errors, from different initial values β_0 of β, group sizes i of magnetometers for localization, meagnetometer sensing noise $\mathcal{N}_1$, camera observation noise $\mathcal{N}_2$. More specifically, the standard deviation of the signal noise is set as a ratio (r_s) of the S_T . In the simulation we choose $r_s = 5\%, 10\%$, the standard deviation of $\mathcal{N}_2 = 0.03, 0.04, ..., 0.10$ distance units respectively, on both X and Y coordinates. respectively.We also investigate how camera sensing can compensate or dilate the location inaccuracy from low-cost magnetometers, under various levels of observation noise.

4.1 Influence of initial value β_0

To evaluate the influence of the initial input β_0 for the nonlinear least square fitting of $\bar{\beta}$, we choose β_0 = 1, 3, 5 ,7, 9. Figure 3 (a) plots the difference of the estimated $\bar{\beta}$ and real β over the number of measurements with r_s = 10% and $i = 8$. As shown in the figure, $\bar{\beta}$ always converges to the same value from different initial values of β_0. For the convergence of $\bar{T}$ to T, similar results under different β_0s are illustrated in figure refbeta0 (b). We have the similar results under r_s = 5%,

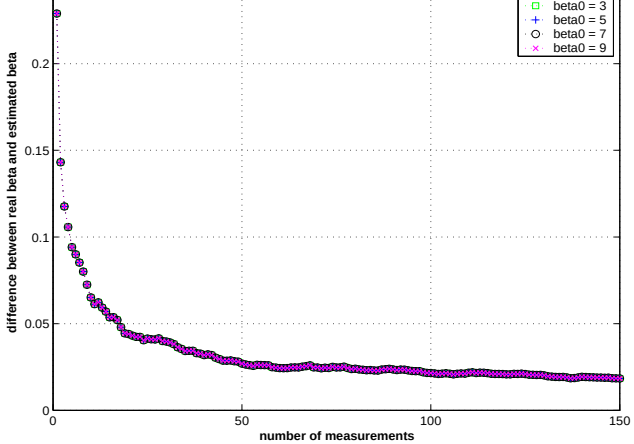

(a)$|\beta - \bar{\beta}|$ when $\mathcal{N}_1 = (0, 0.10S_T)$, $\mathcal{N}_2 = (0, 0)$ and $i = 8$

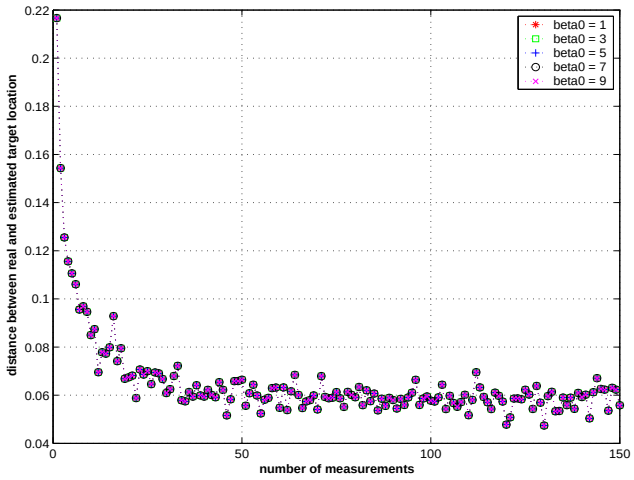

(b)$|T - \bar{T}|$ when $\mathcal{N}_1 = (0, 0.10S_T)$, $\mathcal{N}_2 = (0, 0)$ and $i = 8$

Figure 3: Illustration of the calibration for $\bar{\beta}$ and $\bar{T}$ verse the number of measurements for different β_0 when $\mathcal{N}_1 = (0, 0.10S_T)$, $\mathcal{N}_2 = (0, 0)$ and $i = 8$.

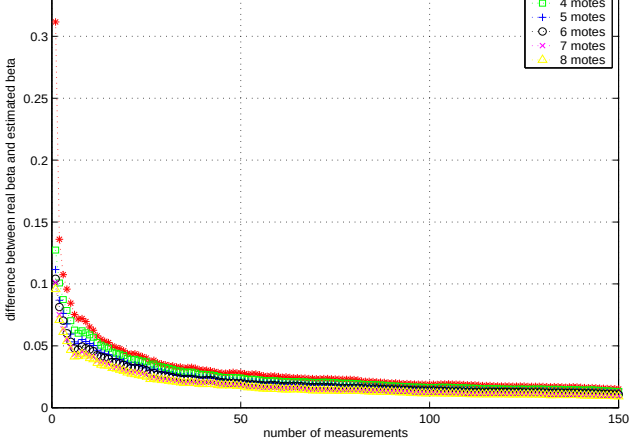

(a)$|\beta - \bar{\beta}|$ when $\mathcal{N}_1 = (0, 0.05S_T)$ and $\mathcal{N}_2 = (0, 0)$

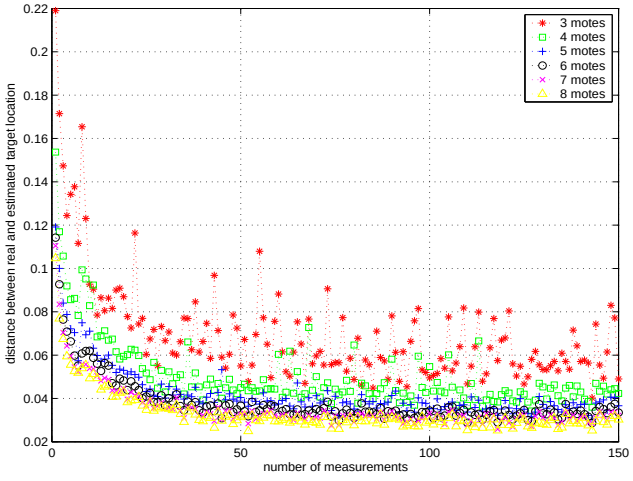

(b)$|T - \bar{T}|$ when $\mathcal{N}_1 = (0, 0.05S_T)$ and $\mathcal{N}_2 = (0, 0)$

Figure 4: Illustration of the calibration for $\bar{\beta}$ and $\bar{T}$ verse the number of measurements for different group size i when $\mathcal{N}_1 = (0, 0.05S_T)$ and $\mathcal{N}_2 = (0, 0)$.

15%, 20%. Therefore, β_0 is set as 3 in the later simulation for simplicity.

4.2 Influence of group size i

Figure 4 (a) illustrates the difference of the estimated $\bar{\beta}$ and real β over the number of measurements for different group size when $\mathcal{N}_1 = (0, 0.05S_T)$ and $\mathcal{N}_2 = (0, 0)$. Figure 4 (b) plots the corresponding location error. It is shown that the estimation for β along becomes more accurate with more sensor readings. Furthermore, the location error decreases with larger group size since we have more accurate $\bar{\beta}$.

Figure 5 (a) plots the difference of the $\bar{\beta}$ and β over the number of measurements for different group size when $\mathcal{N}_1 = (0, 0.05S_T)$ and $\mathcal{N}_2 = (0, 0.10)$. It is also shown that $\bar{\beta}$ is more close to β for larger group size. Figure 5 (b) demonstrates the difference between T and $\bar{T}$ and figure 5 (c) shows the difference between $\tilde{T}$ and $\bar{T}$. Firstly, the location error decreases with more sensor readings because we have more accurate estimation for $\bar{\beta}$. Secondly, there is no noticeable difference between figure 4 (b) and (c). (reason???)

4.3 Influence of signal noise $\mathcal{N}_1$ and camera localization noise $\mathcal{N}_2$

To study the influence of signal noise $\mathcal{N}_1$ to the location error, we do the simulation when there is no signal noise ($\mathcal{N}_1 = (0, 0)$). Figure 6 shows $|\beta - \bar{\beta}|$ error and $|T - \bar{T}|$, $|\tilde{T} - \bar{T}|$ errors for different combinations of signal noise camera localization noise $\mathcal{N}_1$ and camera localization noise $\mathcal{N}_2$.

ferent values, in proportion to $\mathcal{N}_2$'s value, but insensitive to $\mathcal{N}_1$s. Therefore we can conclude that the localization error, in terms of calibration error and target localization error, is mainly contributed by the camera noise $\mathcal{N}_2$.

Moreover, figure 7 illustrates the calibration results for different camera localization noises $\mathcal{N}_2$ when $\mathcal{N}_1 = (0, 0.05S_T)$ and $i = 8$. It is clear that both $\bar{\beta}$ error and $\bar{T}$ error increase with larger $\mathcal{N}_2$.

4.4 Experimental Results

We plan to evaluate our approach on a sensor network testbed that uses MicaZ motes [7] equipped with MTS 310 magnetometers [8] and a camera to track ferrous targets. We expect that coordination across different sensing modalities increases localization accuracy and reduces the amount of imaging data that has to be processed by the network.

5 Related Work

To make sensor devices provide valid and useful readings for sensing detecting and tracking events, we need calibrate their accuracies according to the expected measurement scales [2]. Particularly, [11, 2] address the global calibration problem of large-scale, dense-deployed sensor network using a two-phase collaborative approach [2] or a parameter estimation by optimizing the overall system performance approach [11]. In this paper, the non-imaging sensor devices are calibrated from the estimate of target locations from the direct imaging sensors. This forms a collaborative, heterogeneous sensor network for target detection and localization.

have attracted many research activities in sensor networks. Zou and Chakrabarty [15, 16, 17] propose an energy-aware target detection and localization strategy for cluster-based wireless networks. Rabbat *et. al* [9] present a robust localization algorithm of an isotropic energy source through kernel average over measurements from distributed sensors. Blatt and Hero [1] describe the aggregated projection onto convex sets (APOCS) method by treating the localization problem in its convex feasibility formulation. [1] employ a fast convergent iterative optimization to achieve the global optimum. Li *et. al* [6] estimate target position by solving a non-linear least square problem and assuming that sensors are pre-calibrated. Target localization based on the time-of-arrival (TOA) [5] or the direction-of-arrival (DOA) [12] of acoustical/seismic signals is also explored. Locating victims through emergency sensor networks in a centralized fashion is studied in [10]. In a target is used for target tracking, with target position estimated by the location of the root sensor.

In this paper, we focus on leveraging multi-modal sensor network involving both low-cost non-imaging sensor devices and direct image sensors collaboratively to calibrate the non-image sensor readings, and localize the target position over-time simultaneously.

6 Conclusion

The conclusion goes here.

References

[1] D. Blatt and A.O. Hero, APOCS: a rapidly convergent source localization algorithm for sensor networks, IEEE Workshop on Statistical Signal Processing (SSP), Bordeaux, July 2005

[2] V. Bychkovskiy, S. Megerian, D. Estrin, and M. Potkonjak, "A Collaborative Approach to In-Place Sensor Calibration", IPSN 2003.

[3] X. Cheng, A. Thaeler, G. Xue, and D. Chen, TPS: a time-based positioning scheme for outdoor sensor networks, INFOCOM 2004.

[4] D. Estrin, L. Girod, G. Pottie, and M. Srivastava, Instrumenting the World with Wireless Sensor Networks, *ICASSP'01*, Salt Lake City, UT, 2001.

[5] D. Friedlander, C. Griffin, N. Jacobson, S. Phoha, and R. R. Brooks, Dynamic Agent Classification and Tracking Using an Ad Hoc Mobile Acoustic Sensor Network, *Eurasip Journal on Applied Signal Processing*, 2003:4 (2003) 371-377.

[6] D. Li, K.D. Wong, Y.H. Hu, and A.M. Sayeed, Detection, Classification, and Tracking of Targets, *IEEE Signal Processing Magazine*, Vol. 19, pp. 17-29, March 2002.

[7] http://www.xbow.com/products/productsdetails.aspx?sid=101

[8] http://www.xbow.com/products/productsdetails.aspx?sid=75

[9] M. Rabbat, R. Nowak, and J. Bucklew, Robust decentralized source localization via averaging, IEEE International Conference on Acoustics, Speech, and Signal Processing (ICASSP), 2005.

grini, Ari Trachtenberg, David Starobinski, Robust Location Detection in Emergency Sensor Networks, *IEEE INFOCOM 2003*, San Francisco USA., March 30-April 3, 2003.

[11] K. Whitehouse and D. Culler, "Macro-calibration in Sensor/Actuator Networks", Mobile Networks and Applications Journal (MONET), Special Issue on Wireless Sensor Networks. June, 2003.

[12] L. Yip, K. Comanor, J. C. Chen, R. E. Hudson, K. Yao, and L. Vandenberghe, Array Processing for Target DOA, Localization, and Classification based on AML and SVM Algorithms in Sensor Networks, *2nd International Workshop on Information Processing in Sensor Networks (IPSN'03)*, 2003, Palo Alto, California, USA.

[13] W. Zhang and G. Cao, Optimizing Tree Reconfigration for Mobile Target Tracking in Sensor Networks, *IEEE INFOCOM*, HongKong China, March 2004.

[14] W. Zhang and G. Cao, DCTC: Dynamic Convoy Tree-Based Collaboration for Target Tracking in Sensor Networks, *IEEE Transactions on Wireless Communication*, in press.

[15] Y. Zou, Krishnendu Chakrabarty, Energy-Aware Target Localization in Wireless Sensor Networks, *Proc. of the First IEEE International Conference on Pervasive Computing and Communications*, 23-26 March 2003, Pages:60 - 67.

[16] Y. Zou, Krishnendu Chakrabarty, Target Localization Based on Energy Considerations in Distributed Sensor Networks, *Proc. of the First IEEE International Workshop on Sensor Network Protocols and Applications*, 11 May 2003, Pages:51 - 58.

[17] Y. Zou, Krishnendu Chakrabarty, Sensor Deployment and Target Localization in Distributed Sensor Networks, *ACM Transactions on Embedded Computing Systems*, Vol. 3, No. 1, February 2004, Pages 61-91.

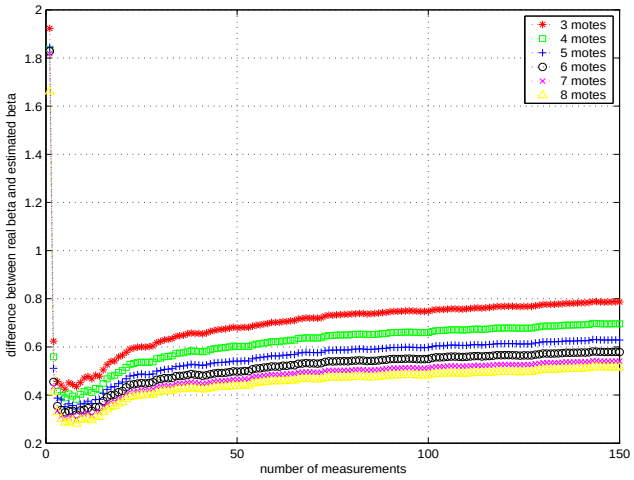

(a)$|\beta - \bar{\beta}|$ when $\mathcal{N}_1 = (0, 0.05S_T)$ and $\mathcal{N}_2 = (0, 0.10)$

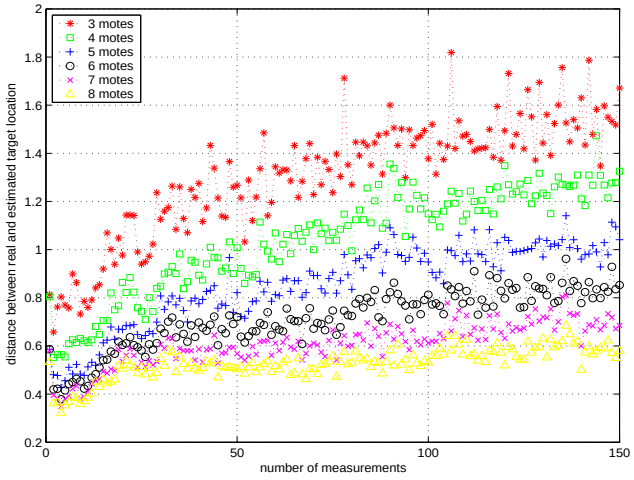

(b)$|T - \bar{T}|$ when $\mathcal{N}_1 = (0, 0.05S_T)$ and $\mathcal{N}_2 = (0, 0.10)$

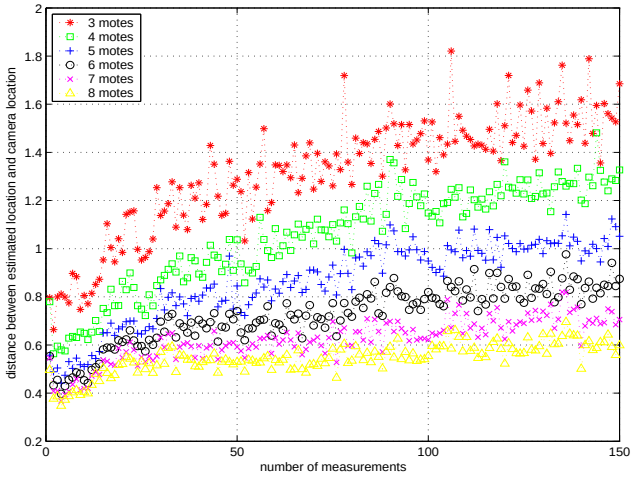

(c)$|\tilde{T} - \bar{T}|$ when $\mathcal{N}_1 = (0, 0.05S_T)$ and $\mathcal{N}_2 = (0, 0.10)$

Figure 5: Illustration of the calibration errors, $|\beta - \bar{\beta}|$, $|T - \bar{T}|$ and $|\tilde{T} - \bar{T}|$, of $\bar{\beta}$ and $\bar{T}$ verse the number of measurements for different group size i when $\mathcal{N}_1 = (0, 0.05S_T)$ and $\mathcal{N}_2 = (0, 0.10)$.

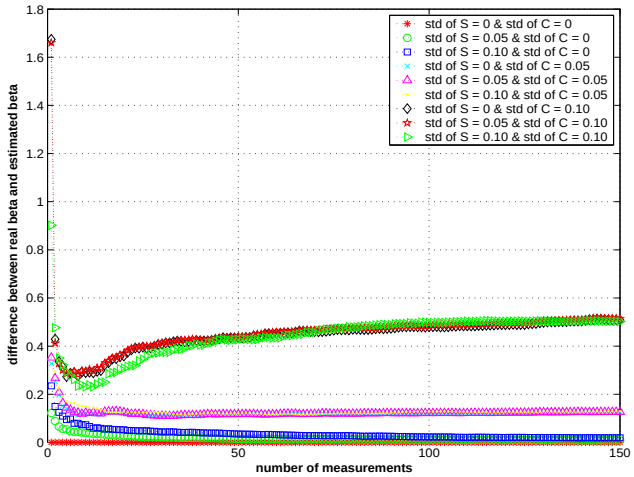

(a)$|\beta - \bar{\beta}|$ for different $\mathcal{N}_1$ and $\mathcal{N}_2$ when $i = 8$

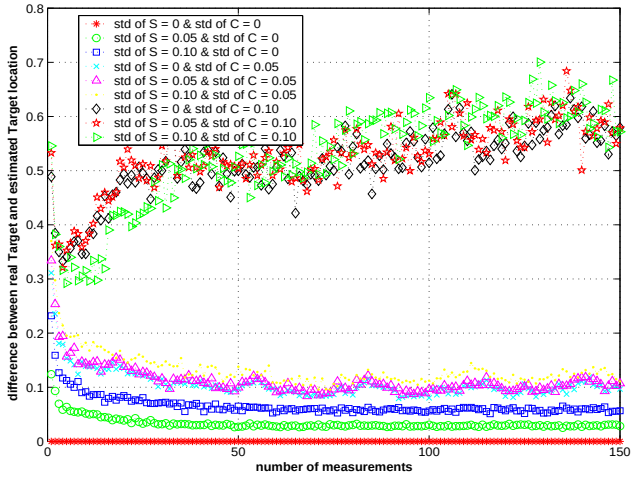

(b)$|T - \bar{T}|$ for different $\mathcal{N}_1$ and $\mathcal{N}_2$ when $i = 8$

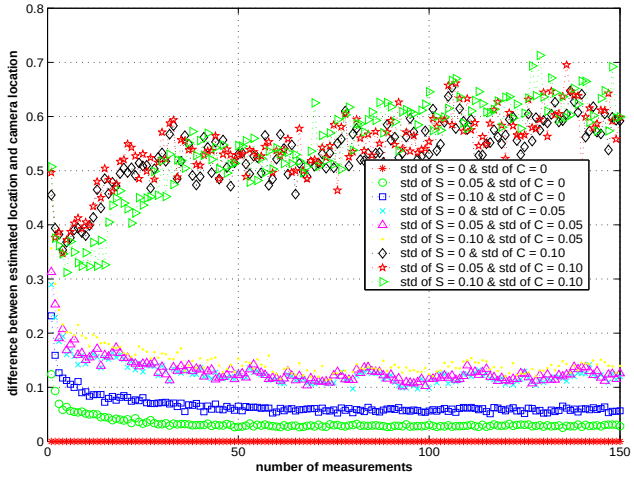

(c)$|\tilde{T} - \bar{T}|$ for different $\mathcal{N}_1$ and $\mathcal{N}_2$ when $i = 8$

Figure 6: Illustration of the calibration errors, $|\beta - \bar{\beta}|$, $|T - \bar{T}|$ and $|\tilde{T} - \bar{T}|$, of $\bar{\beta}$ and $\bar{T}$ verse the number of measurements for different combinations of $\mathcal{N}_1$ and $\mathcal{N}_2$ when $i = 8$.

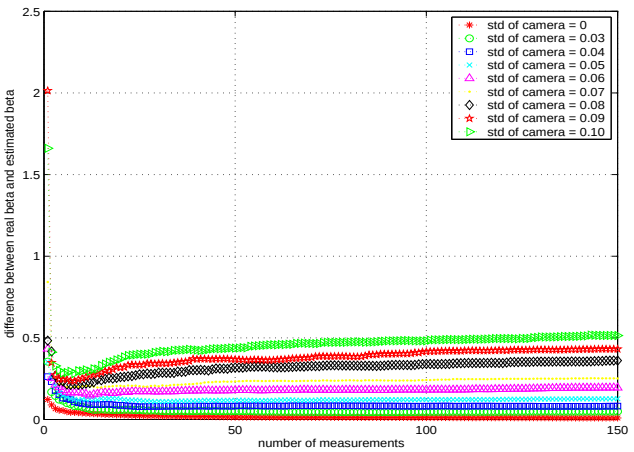

(a)$|\beta - \bar{\beta}|$ for different $\mathcal{N}_2$ when $\mathcal{N}_1 = (0, 0.05S_T)$ and $i = 8$

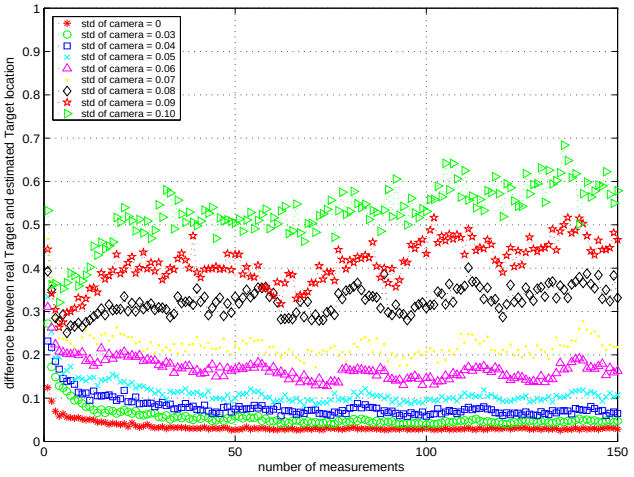

(b)$|T - \bar{T}|$ for different $\mathcal{N}_2$ when $\mathcal{N}_1 = (0, 0.05S_T)$ and $i = 8$

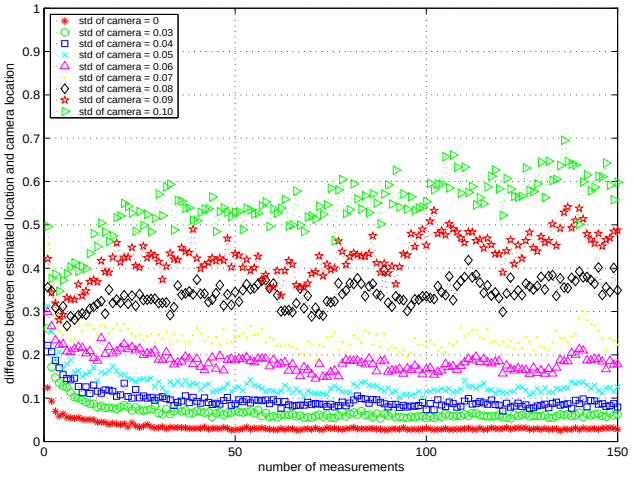

(c)$|\tilde{T} - \bar{T}|$ for different $\mathcal{N}_2$ when $\mathcal{N}_1 = (0, 0.05S_T)$ and $i = 8$

Figure 7: Illustration of the calibration errors, $|\beta - \bar{\beta}|$, $|T - \bar{T}|$ and $|\tilde{T} - \bar{T}|$, of $\bar{\beta}$ and $\bar{T}$ verse the number of measurements for different $\mathcal{N}_2$ when $\mathcal{N}_1 = (0, 0.05S_T)$ and $i = 8$.